

## An analysis of the evaluation of the fracture energy using the DCB-specimen

A. BIEL, U. STIGH

*University of Skövde  
SE-541 28 Skövde, Sweden*

THE METHODS TO ESTIMATE the fracture energy using DCB-specimens as advocated in common standards. For instance, ASTM D 3433 and BS 7991:2001 are based on a compliance method, i.e. on linear elastic fracture mechanics (LEFM). Since the mechanical properties of almost all adhesives are non-linear, errors are generated. In some of the standards, the non-linear behaviour is compensated for by the use of correction terms generated from the experiments. An analysis of the methods of evaluation the fracture energy from experiments is performed. This analysis is performed first by simulating an experiment using realistic data for an engineering adhesive and then, by analysing the results with different methods. In this way, the correct fracture energy is known beforehand and the error in the evaluated fracture energy can be determined. In the present work it is shown that the magnitude of this error depends on the length of the crack. The results show that some commonly used methods generate substantial errors when a large region of non-linear deformation precedes the crack tip. It is also shown that methods based on nonlinear fracture methods do not produce this kind of error.

### 1. Introduction

THE DCB GEOMETRY is a very common test specimen for studies of strength of adhesives and delamination of composites. The geometry and notation for a DCB-specimen are given in Fig. 1. Several methods have been developed to analyse the specimen. The two main principles are based on linear and non-linear fracture mechanics. In this paper, for the methods that assume the specimen to be linear elastic, the fracture energy is denoted  $G_C$  and for the methods that consider the nonlinear behaviour, the fracture energy is denoted  $J_C$ .

The foundation of the methods based on linear elastic fracture mechanics is developed in [1]. For a linear structure, the fracture energy is given by

$$(1.1) \quad G_C = \frac{F^2}{2b} \frac{\partial C}{\partial a}$$

where  $C \equiv \Delta/F$  is the compliance of the specimen and  $a$  is the crack length. The differences between the different methods depend on how the differentiation of



This is the basis for most standards. Three alternative expressions of the fracture energy can be obtained by means of Eq. (1.2), cf. [4].

$$(1.4) \quad G_{C,UB2}(F, a, \Delta) = \frac{3F\Delta}{2ba},$$

$$(1.5) \quad G_{C,UB3}(F, \Delta) = \frac{F^2}{EIb} \left( \frac{3EI\Delta}{2F} \right)^{2/3},$$

$$(1.6) \quad G_{C,UB4}(a, \Delta) = \frac{9EI\Delta^2}{4ba^4}.$$

Equations (1.3) to (1.6) have a varying sensitivity for the measurement of the crack length. Equation (1.5) is independent of the crack length but needs a measurement of the deflection at the loading point. Equation (1.6) is used to analyse the cleavage test where  $\Delta$  is given by the thickness of the wedge. Obviously, it needs an accurate measurement of the crack length. Since both the wedge and the tip of the crack are moving during an experiment this measurement may be difficult. It is also worth to notice that this equation is independent of the friction between the wedge and the adherends.

In [5], MOSTOVOY *et al.* use the Timoshenko beam theory to determine the compliance, i.e. the full expression in Eq. (1.2). With  $C \equiv \Delta/F$ ,  $G = E/2(1+\nu)$  and Poisson's ratio  $\nu = 1/3$ , the fracture energy is

$$(1.7) \quad G_{C,SB}(F, a) = \frac{4F^2}{Eb^2} \left[ \frac{3a^2}{h^3} + \frac{1}{h} \right] = \frac{12F^2a^2}{Eb^2h^3} \left( 1 + \frac{1}{12} \left( \frac{h}{a} \right)^2 \right),$$

where the second term in the parenthesis of the last expression is identified as the compensation due to shear deformation of the adherends. As apparent, the effect of shear deformation of the adherends is important if  $a$  is small in comparison with  $h$ . If  $h = 1.1a$  the fracture energy evaluated by Eq. (1.7) is about 10% larger than that evaluated by Eq. (1.3).

To compensate for the rotation of the adherends at the crack tip and for the flexibility of the adhesive layer, the crack length is sometimes increased with a correction term  $\delta$ , cf. e.g. [6]. According to the Euler–Bernoulli beam theory and with the corrected crack length  $(a + |\delta|)$ , the compliance is given by

$$(1.8) \quad C(a) = \frac{8}{Eb} \frac{(a + |\delta|)^3}{h^3}.$$

Since the compliance contains  $(a + |\delta|)^3$  the correction term,  $|\delta|$ , is given as a segment on the  $a$ -axis in a plot of the experimental compliance,  $C^{1/3}$  vs. the crack length  $a$ , cf. Fig. 2. This method is used experimentally to determine  $|\delta|$ . Differentiating Eq. (1.8), the fracture energy is given by

$$(1.9) \quad G_{C,CLC}(F, a, \Delta) = \frac{3F\Delta}{2b(a + |\delta|)}.$$

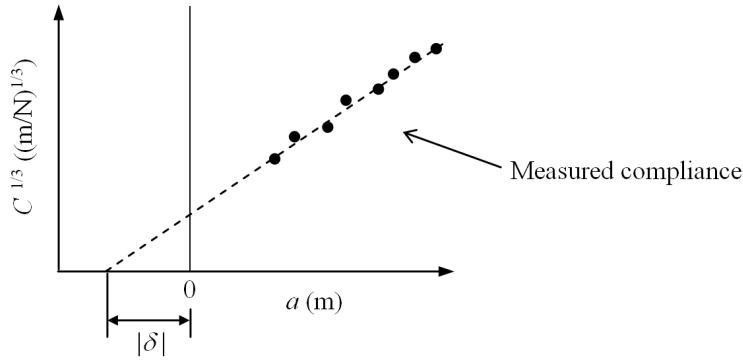


FIG. 2. Plot of the cubic root of the compliance vs. the crack length.

The same principle can be used with Timoshenko beam theory, cf. Eq. (1.7) and e.g. [7]. By taking  $\nu \equiv 1/3$ , the fracture energy is

$$(1.10) \quad G_{C,SCC}(F, a) = \frac{4F^2}{Eb^2} \left( \frac{3(a + |\delta|)^2}{h^3} + \frac{1}{h} \right).$$

According to [7],  $|\delta| \approx h/3$  from experiments.

BERRY [8] proposes to determine the compliance by an empirical approach. This method is directly based on Eq. (1.1). The compliance is approximated by a power law,

$$(1.11) \quad C = ka^n$$

where  $n$  and  $k$  are determined experimentally. Differentiation yields after some manipulation,

$$(1.12) \quad G_{C,EC} = \frac{nF\Delta}{2ba}.$$

The exponent  $n$  is determined experimentally by plotting  $\log C$  vs.  $\log a$ , cf. Fig. 3. It can be noted that according to the Euler–Bernoulli beam theory, with the adherends assumed as clamped at the beginning of the adhesive layer,  $n = 3$ . Alternative methods used to empirically determine the fracture energy by power laws are given in [9].

An alternative method to evaluate the DCB-specimen is to use the concept of energetic forces introduced in [10]. This concept was developed to the two-

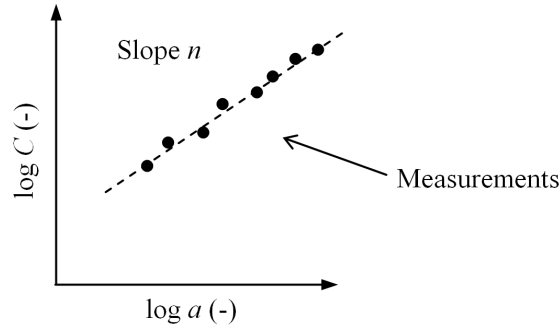


FIG. 3. Plot of the logarithm of the compliance vs. the logarithm of the crack length.

dimensional  $J$ -integral approach in [11]. The  $J$ -integral is given by

$$(1.13) \quad J = \int_S \left( W dy - \mathbf{T} \cdot \frac{\partial \mathbf{u}}{\partial x} ds \right)$$

where  $W$  is the strain energy density,  $\mathbf{u}$  is the displacement vector, and  $\mathbf{T}$  is the traction vector acting on the area  $S$  circumscribing the crack tip. PARIS and PARIS [12] use the integral to evaluate  $J$  for a DCB-specimen. By assuming the applied forces to be distributed over a small horizontal increment  $dx$ , the energy release rate is derived as

$$(1.14) \quad J = \frac{2F\theta}{b}.$$

The same result has been derived in two similar analyses. In [13], STIGH and ANDERSSON derive the result directly based on the concept of equilibrium of energetic forces. In [14], ANDERSSON and STIGH use the  $J$ -integral and the Euler-Bernoulli beam theory. The result is also implicit in [15] and has recently been extended to large deformations in [16]. An important requirement for Eq. (1.14) to provide the energy release rate is that the material acts as if it was elastic. This is often the case if no material point is subject to unloading from an inelastically deformed state. If effects of unloading from an inelastic state can be ignored, Eq. (1.14) gives a good estimate of the energy release rate. Since  $a$  does not appear in Eq. (1.14), it can be used to measure the instantaneous value of the fracture energy,  $J_C$ , during crack propagation.

It can be noted here that since the energy release rate can be evaluated instantaneously from Eq. (1.14) and since there is a close connection between the stress-elongation relation and the energy release rate, there is an opportunity

to determine the stress-elongation relation for the adhesive layer. In this way STIGH and ANDERSSON [14]<sup>2)</sup> derive,

$$(1.15) \quad \sigma(w) = \frac{2}{b} \frac{d(F\theta)}{d} w$$

where  $w$  is the elongation of the adhesive layer at the beginning of the adhesive layer, cf. Fig. 1. A similar approach, but with moments applied instead of forces, has been used in [17]. In [3, 13] experimental results evaluated by means of Eq. (1.15) are reported. These results are used in the present paper to model the behaviour of the adhesive.

As compared to the methods based on LEFM, these methods are exact providing a unique strain energy density for the adhesive layer and the problem can be considered as two-dimensional.

## 2. Standards

The use of standards, for instance, the British Standard BS7991 [18] and the ASTM D 3433 [19], is very common when analysing the fracture energy of adhesive layers. Similar standards have also been developed for delamination in composites. The standards propose different methods to evaluate the fracture energy. All these methods are based on LEFM. Table 1 summarise the equations used in each standard. The British Standard BS7991 insists that all the methods should be used if possible. Equations (1.9) and (1.12) are assumed to give a better accuracy than Eq. (1.7). It is argued that since Eqs. (1.9) and (1.12) are based on linear plots, only Eq. (1.7) should be used if stick-slip occurs during crack propagation.

**Table 1. Equations used in the standards.**

ASTM D 3433 (1999)	Use Eq. (1.7). This standard is based on the geometry given in Fig. 5.
British Standard BS 7991 (2001)	Use Eq. (1.7), Eq. (1.9), and Eq. (1.12). The two latter methods are considered to be the most accurate. According to this standard, a non-adhesive insert (PTFE-film) is put in the adhesive to initiate the crack. This insert shall be thinner than 13 $\mu\text{m}$ .

## 3. Comparison between different methods of evaluation

In order to make an investigation of the different methods to evaluate experiments with the DCB-specimen, a FE-simulation is first made with the adhesive

<sup>2)</sup>It should be noted that Eq. (1.15) was originally derived by OLSSON and STIGH [15].

layer represented by non-linear springs, with a force-elongation relation adopted to reflect the stress-elongation relation determined from the experiments, cf. Figs. 4 to 6 and [3]. Simulations show that the adhesive at the beginning of the layer experiences a monotonically increasing elongation. However, at some distance into the layer, the adhesive first experiences compression and later, when the crack starts to propagate, elongation. In the simulations, the maximum compressive stress is always less than 18 MPa, i.e. less than the level giving non-linear behaviour of the adhesive. Thus, the full constitutive behaviour of the adhesive incorporating unloading from an inelastic state needs not to be known for the present study.

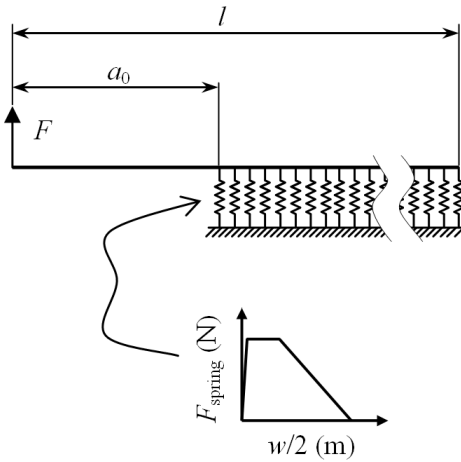


FIG. 4. FE-model of the upper part of the specimen.

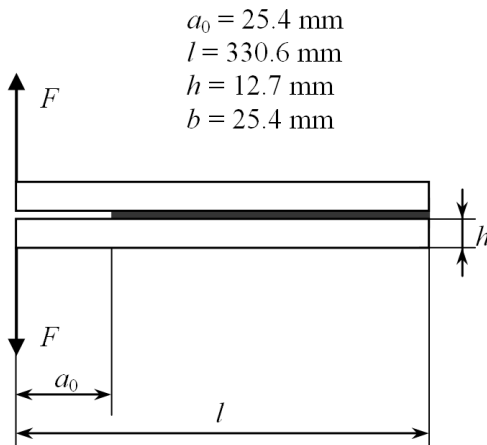


FIG. 5. The geometry according to ASTM D 3433.

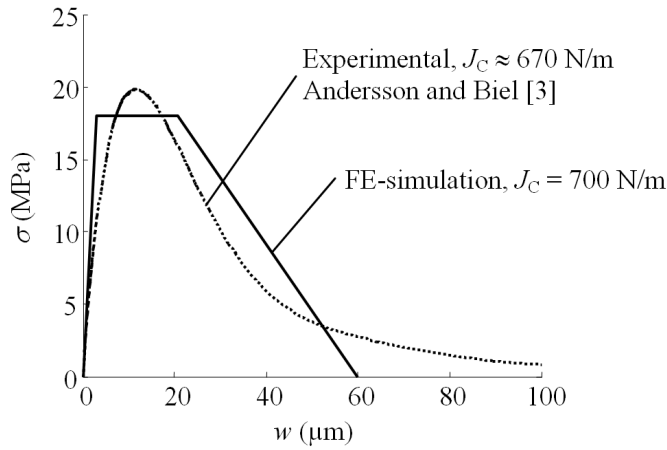


FIG. 6. Stress elongation relation from experiments and adopted for numerical analysis.

As an alternative to the use of spring elements, cohesive elements can be used. However, cohesive elements with Newton–Cotes integration are numerically equivalent to spring elements and we prefer the use of nonlinear springs in this study. In previous studies it has been shown that FE-simulations give good accuracy as compared to experimental results, cf. [3, 13, 14]. With this procedure, the correct fracture energy is known a priori;  $J_C = 700$  N/m. The FE-model consists of 3394 elastic beam elements with  $E = 213$  GPa and 3138 spring elements. The distance between the spring elements is 0.1 mm. This distance is very small as compared to the length of the damage zone, here defined as the distance from the crack tip to the first element behaving linearly elastic. The maximum crosshead displacement,  $\Delta_{\max}$ , is set to 6 mm in the analysis which corresponds to a substantial crack growth during the simulation. The result of the FE-analysis is used to evaluate the fracture energy by use of all the experimental methods presented above. The geometry is chosen according to the recommendation in ASTM D 3433, cf. Fig. 5. This geometry is also acceptable according to British Standard BS7991. Figures 7 to 12 show the results of the simulation.

Figure 12 shows the force vs. the length of the damage zone. As previously mentioned, the damage zone is defined as the part of the adhesive layer where the adhesive behaves nonlinearly, i.e. for the present model,  $w$  is between 3  $\mu\text{m}$  and 60  $\mu\text{m}$ . Up to an applied force of about 500 N the adhesive deforms elastically. With increasing loading, the length of the damage zone increases until the crack starts to propagate. During crack propagation the length of the damage zone decreases.

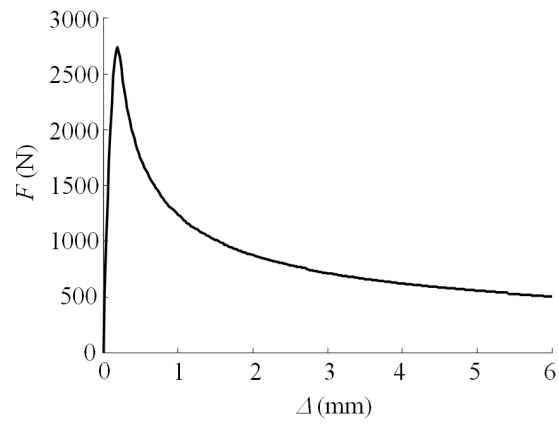


FIG. 7. Force vs. displacement at the loading point.

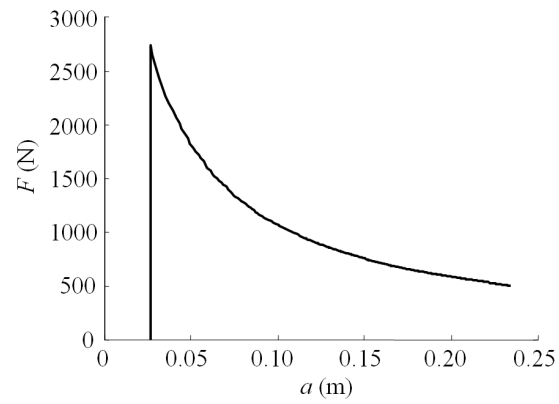


FIG. 8. Force vs. crack length during crack propagation.

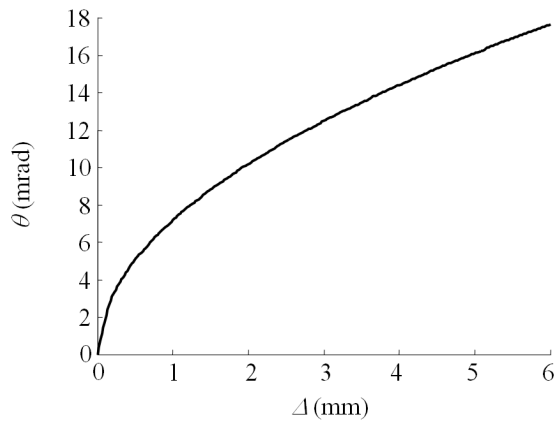


FIG. 9. Rotation vs. displacement at the loading point.

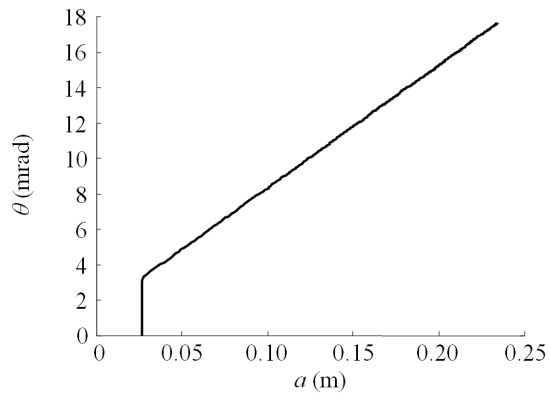


FIG. 10. Rotation vs. crack length during crack propagation.

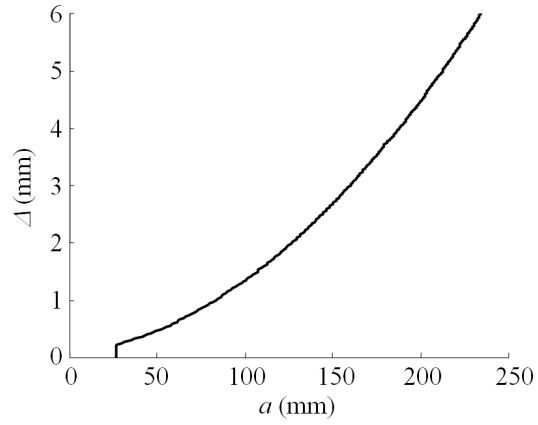


FIG. 11. Displacement vs. crack propagation.

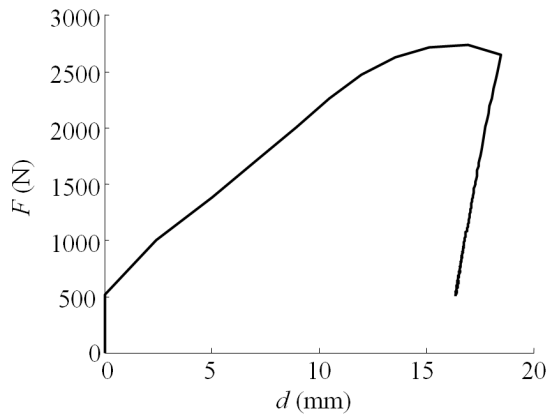


FIG. 12. Force vs. length of damage zone.

### 3.1. Evaluation by the methods based on LEFM

These methods accounts only for the flexibility of the adherends between the crack tip and the loading point.

**3.1.1. Compliance determined by the beam theory.** Five different methods to evaluate the fracture energy are based on the beam theory where the adherends are assumed to be clamped at the beginning of the adhesive layer. Four of these, Eqs. (1.3) to (1.6), are based on the Euler-Bernoulli beam theory and one on the shear-corrected Timoshenko beam theory, Eq. (1.7). Using the simulated experimental result and these methods, the evaluated fracture energy is given in Fig. 13.

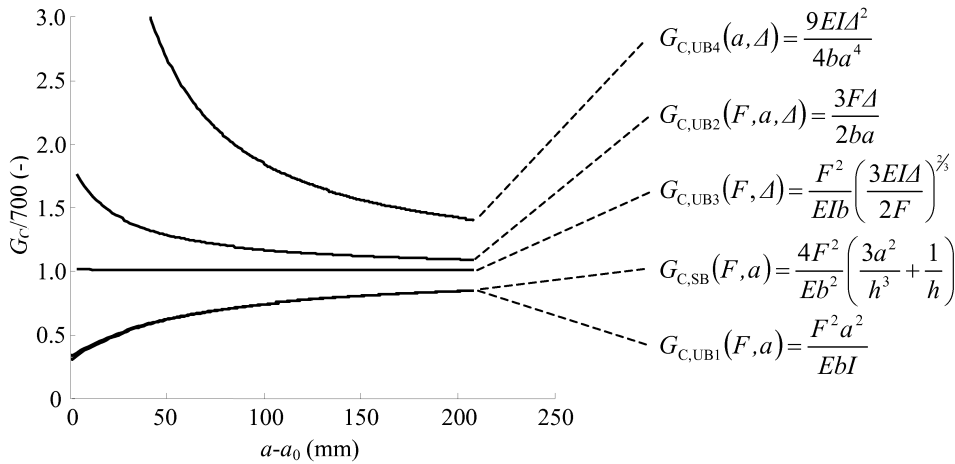


FIG. 13. Normalised fracture energy vs. crack length for a propagating crack. Evaluation based on the beam equations (note:  $G_{C,SB}$  and  $G_{C,UB1}$  do almost coincide).

It is noted that only one of these methods,  $G_{C,UB3}$  provides a stable value of the fracture energy, i.e. a value that does not vary with crack propagation. It is interesting to note that this expression for the fracture energy is independent of the crack length. Thus, a virtual crack extension as suggested in Eqs. (1.9) to (1.10) does not contribute to the expression since  $a$  is not present. One may also expect that the variation of fracture energy with crack propagation which is sometimes reported, i.e. the  $R$ -curve, might be an effect of errors in the method of evaluation if some of the other methods are used.

For the present specimen, the difference is very small between the shear corrected beam theory,  $G_{C,SB}$  and the uncorrected beam theory  $G_{C,UB1}$ . Thus, the influence of the shear deformation is insignificant. The equation for  $G_{C,UB3}$  which does not contain the crack length, evidently gives the best accuracy. The

figure clearly shows that other methods for evaluating the fracture energy are not able to determine the correct value.

**3.1.2. Compliance determined by the beam theory and a correction term.** These methods are based on Eqs. (1.9) and (1.10). They are based on the Euler-Bernoulli or Timoshenko beam theory and a correction term corresponding to an increase in the crack length. The correction term for the method that is based on the Euler-Bernoulli beam theory, is determined by a plot of the cubic root of the compliance vs. the crack length. The result of the simulation is given in Fig. 14. For this geometry and adhesive, the length correction is about 22 mm.

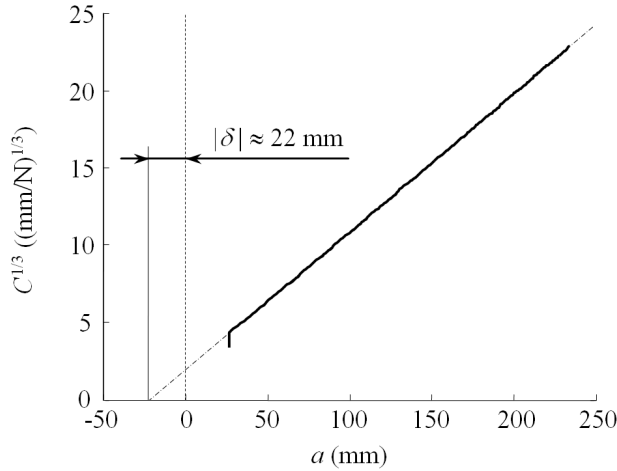


FIG. 14. Cubic root of the compliance vs. the crack length.

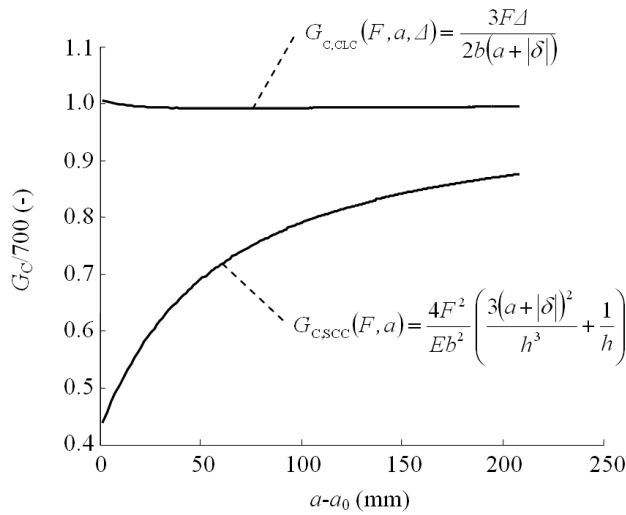


FIG. 15. Normalised fracture energy vs. crack length propagation.

The evaluated fracture energies vs. the crack length for these two methods are given in Fig. 15. Using the method based on the Timoshenko beam theory, the correction term is taken as  $h/3$ , as suggested in [7].

The accuracy is better than 2 % for the method based on the Euler–Bernoulli beam theory. The error is larger than 40 % for the method based on Timoshenko beam theory for short crack lengths. The methods are sensitive to the choice of correction term. If the fracture toughness is varying along the adhesive layer or if only a few measurements are collected, it is difficult to make a good estimate of the correction term by a linear fit, cf. e.g. [4].

**3.1.3. Compliance determined by empirical approaches.** The fracture energy determined by Eq. (1.12) requires that a linear fit should be made to the logarithm of the compliance vs. the logarithm of the crack length. This plot is presented in Fig. 16. For this specific case, the slope is determined to be 2.1. An alternative value is given by the use of the instantaneous slope  $n(a)$ . The fracture energies from both methods are presented in Fig. 17. Using the linear fit, the fracture energy is overestimated for short crack lengths and underestimated for long crack lengths. The accuracy of the tested geometry and crack lengths is better than 20 %. The accuracy is increased by use of the instantaneous slope. However, this method appears to be difficult to use experimentally considering scatter in the fracture energy along the adhesive layer.

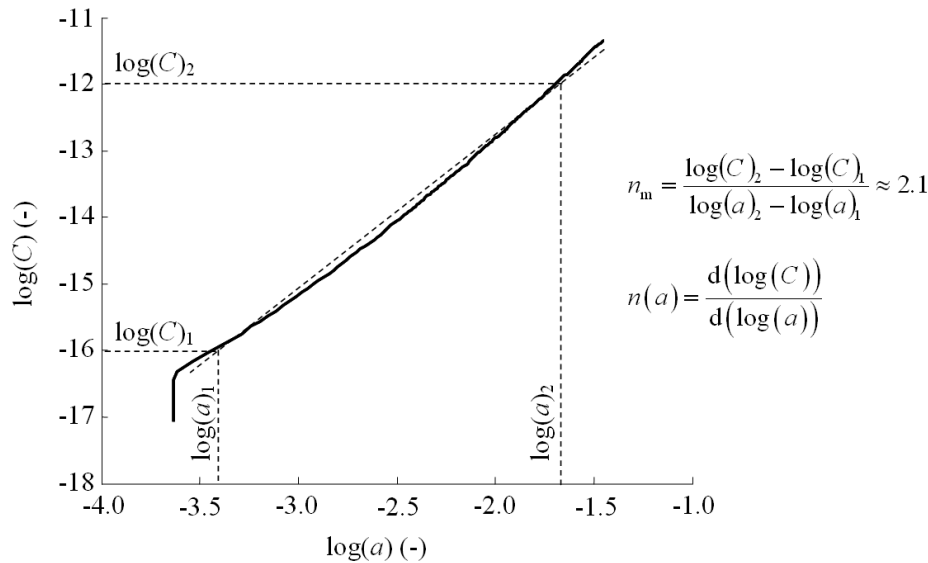


FIG. 16. Logarithm of the compliance vs. logarithm of the crack length and an approximation of the slope.

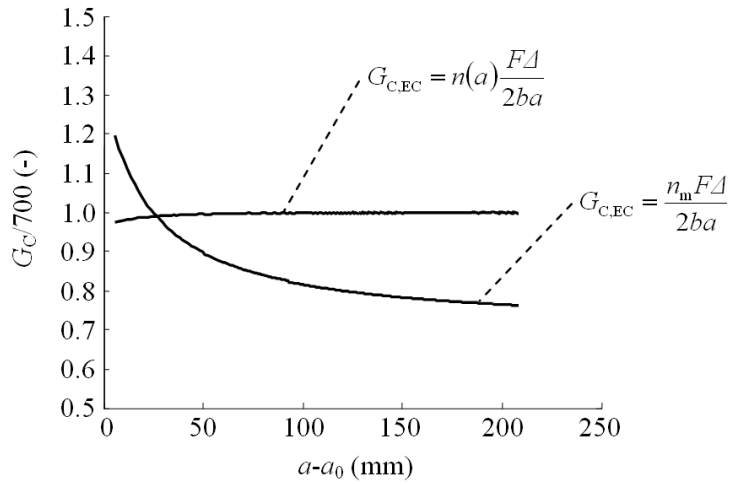


FIG. 17. Normalised fracture energy vs. crack length for a propagating crack.

### 3.2. Methods based on non-linear fracture mechanics

This method is based on Eq. (1.14). Theoretically, this method should generate the fracture energy 700 N/m independently of the crack length. The result of the analysis made with this method is shown in Fig. 18. The deviation is

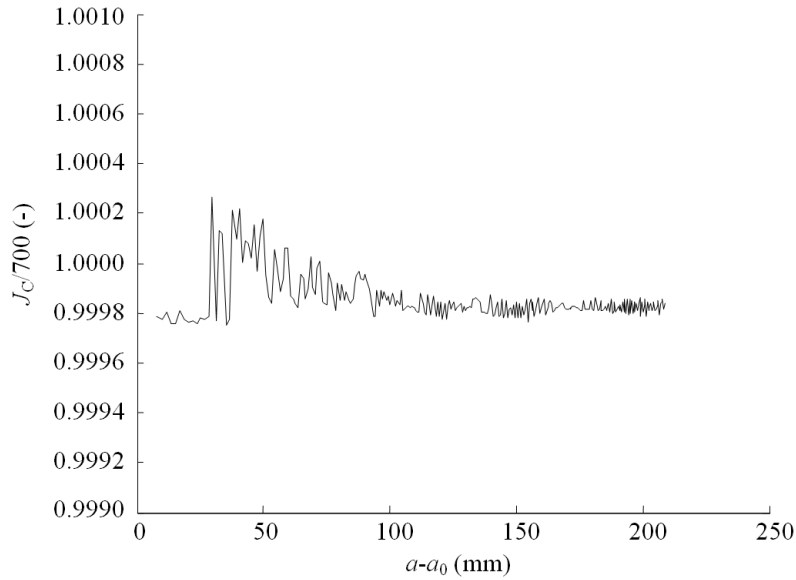


FIG. 18. Normalised fracture energy vs. the crack length for a propagating crack.

smaller than all the other methods. The deviation is due to numerical errors in the FE-simulation. It should be noted that the rotation  $\theta$  in Eq. (1.14) is the rotation of the neutral axis of the beam, which differs from the rotation of the cross-section due to shear deformation.

#### 4. Conclusion

A number of methods are available to evaluate the fracture properties of adhesives obtained by experiments using the DCB-specimen. Most of these methods are based on LEFM and most of them need an accurate measurement of the length of the crack. Since the fracture process almost always leads to the nucleation of multiple micro-cracks in a long damage zone heading the crack tip, this measurement is difficult to do. Moreover, these micro-cracks often appear at several points across the thickness of the layer. These micro-cracks make it virtually impossible to locate the crack tip during an experiment.

The comparison of methods used for evaluation of the fracture energy from the experiments shows that many of the methods lead to large errors of the fracture energy. However, the British Standard BS7991, [18], provides one method that gives small errors; smaller than 2% for the present adhesive, cf. Eq. (1.9). The two other methods give errors larger than 20%. It is also noted that one of the methods suggested by TAMUZS *et al.* [4] gives good accuracy; the error is smaller than 1.5%, cf. Eq. (1.5). For the method presented in ASTM D3433 [19], the error for short crack propagation,  $a - a_0 < 50$  mm, is larger than 40%.

It is doubtful if the standards can be used with any confidence for modern tough engineering adhesives. Curves similar to the ones shown in Figs. 13 and 17 can be obtained by analysing DCB-specimens with these methods, cf. e.g. [20].

The use of methods based on nonlinear fracture mechanics is shown to be superior to all the other methods, cf. Eq. (1.14). In principle this is due to two properties of the method: it is theoretically exact and there is no need to measure the crack length.

In the evaluations of the simulated experiment, no consideration has been given to the errors of measurement. It should be stressed that the crack tip is very often difficult to localize in an experiment and the methods relying on an accurate value of the crack length may lead to large errors. Considering these arguments, the methods based on expressions without the crack length, i.e. Eqs. (1.5) and (1.14), are recommended. However, Eq. (1.5) depends explicitly on the bending stiffness of the adherends, i.e. the beam height raised to the third power. This means that a small error in the measurement of the beam height leads to large errors in the evaluated fracture energy.

## References

1. G. R. IRWIN and J. A. KIES, *Critical energy rate analysis of fracture strength*, Weld. J., **33**, Welding Research Supplement, 193–198, 1954.
2. J. P. SARGENT, *Durability studies for aerospace applications using modulus I and wedge tests*, International Journal of Adhesion and Adhesives, **25**, 247–256, 2005.
3. T. ANDERSSON and A. BIEL, *On the effective constitutive properties of a thin adhesive layer loaded in peel*, International Journal of Fracture, **141**, 227–246, 2006.
4. V. TAMUZS, S. TARASOV and U. VILKS, *Delamination properties of trans laminar-reinforced composites*, Composites Science and Technology, **63**, 1423–1431, 2003.
5. S. MOSTOVOY, P. B. CROSLLEY and E. J. RIPLING, *Use of Crack-Line-Loaded Specimens for Measuring Plane-Strain Fracture Toughness*, Journal of Materials, **2**, 661–668, 1967.
6. J. G. WILLIAMS, *The fracture mechanics of delamination tests*, The Journal of Strain Analysis for Engineering Design, **24**, 4, 207–214, 1989.
7. H. TADA, P. C. PARIS and G. R. IRWIN, *The stress analysis of cracks handbook*, ASME Press, New York 2000.
8. J. P. BERRY, *Determination of fracture surface energies by the cleavage technique*, Journal of Applied Physics, **34**, 62–68, 1963.
9. K. KAGEYAMA and M. HOJO, *Proposed Methods for Interlaminar Fracture Toughness Tests of Composite Laminates*, Proceedings of the 5-th U.S./Japan Conference on Composite Materials, Tokyo, 1990, 227–234, 1990.
10. J. D. ESHELBY, *The force on an elastic singularity*, Phil. Trans. R. Soc., London, **A244**, 87–112, 1951.
11. J. R. RICE, *A path-independent integral and the approximation analysis of the concentration by notches and cracks*, Journal of Applied Mechanics, **35**, 379–386, 1968.
12. A. J. PARIS and P. C. PARIS, *Instantaneous evaluation of  $J$  and  $C^*$* , International Journal of Fracture, **38**, 19–21, 1988.
13. U. STIGH and T. ANDERSSON, *An experimental method to determine the complete stress-elongation relation for a structural adhesive layer loaded in peel*, [in:] Fracture of Polymers, Composites and Adhesives, J.G. WILLIAMS and A. PAVAN [Eds.],ESIS publication **27**, 297–306, 2000.
14. T. ANDERSSON, and U. STIGH, *The stress-elongation relation for an adhesive layer loaded in modulus I using equilibrium of energetic forces*, International Journal of Solids and Structures, **41**, 413–434, 2004.
15. P. OLSSON and U. STIGH, *On the determination of the constitutive properties of the interphase layers – an exact solution*, International Journal of Fracture, **41**, 71–76, 1989.
16. F. NILSSON, *A tentative method for determination of cohesive zone properties in soft materials*, International Journal of Fracture, **136**, 133–142, 2005.
17. B. F. SØRENSEN, *Cohesive law and notch sensitivity of adhesive joints*, Acta Materialia, **50**, 1053–1061, 2002.

18. British Standard BS7991:2001. 2001. *Determination of the mode I adhesive fracture energy  $G_{IC}$  of structure adhesives using the double cantilever beam (DCB) and tapered double cantilever beam (TDCB) specimens*, British Standard Institution, London, Great Britain.
19. ASTM D 3433 1999. Fracture strength in cleavage of adhesives in bonded joints. American Society for Testing and Materials, Philadelphia, USA.
20. I. A. ASHCROFT, *International Journal of Adhesion and Adhesives*, **21**, 87–99, 2001.

*Received December 12, 2006; revised version February 26, 2007.*

---